Large Molecular Weight Nitroxide Biradicals Providing Efficient Dynamic Nuclear Polarization at Temperatures up to 200 K

Alexandre Zagdoun,[†] Gilles Casano,[∥] Olivier Ouari,[∥] Martin Schwarzwälder,[‡] Aaron J. Rossini,[†] Fabien Aussenac,[§] Maxim Yulikov,[‡] Gunnar Jeschke,[‡] Christophe Copéret,[‡] Anne Lesage,[†] Paul Tordo,*,[∥] and Lyndon Emsley*,[†]

[†]Centre de RMN à Très Hauts Champs, Institut de Sciences Analytiques, Université de Lyon (CNRS/ENS Lyon/UCB Lyon 1), 69100 Villeurbanne, France

[∥]Aix-Marseille Université, CNRS, ICR UMR 7273, 13397 Marseille, France

[‡]Department of Chemistry, ETH Zürich, CH-8093, Zürich, Switzerland

[§]Bruker BioSpin SA, Wissembourg, 67160, France

ⓢ *Supporting Information*

ABSTRACT: A series of seven functionalized nitroxide biradicals (the bTbK biradical and six derivatives) are investigated as exogenous polarization sources for dynamic nuclear polarization (DNP) solid-state NMR at 9.4 T and with ca. 100 K sample temperatures. The impact of electron relaxation times on the DNP enhancement (ε) is examined, and we observe that longer inversion recovery and phase memory relaxation times provide larger ε. All radicals are tested in both bulk 1,1,2,2-tetrachloroethane solutions and in

mesoporous materials, and the difference in ε between the two cases is discussed. The impact of the sample temperature and magic angle spinning frequency on ε is investigated for several radicals each characterized by a range of electron relaxation times. In particular, TEKPol, a bulky derivative of bTbK with a molecular weight of 905 g·mol^{-1}, is presented. Its high-saturation factor makes it a very efficient polarizing agent for DNP, yielding unprecedented proton enhancements of over 200 in both bulk and materials samples at 9.4 T and 100 K. TEKPol also yields encouraging enhancements of 33 at 180 K and 12 at 200 K, suggesting that with the continued improvement of radicals large ε may be obtained at higher temperatures.
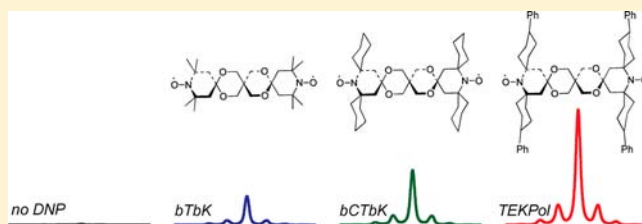
■ INTRODUCTION

Dynamic nuclear polarization (DNP)[1,2] is currently one of the most efficient methods to increase the sensitivity of NMR experiments. Nuclear polarization can be enhanced by microwave (MW) induced polarization transfer from unpaired electrons, with a theoretical limit for the signal enhancement of $\varepsilon_{max} = \gamma_e/\gamma_X$, where γ_e and γ_X are the gyromagnetic ratios of the electron and of the target nuclei, respectively ($\varepsilon_{max} = 660$ for proton, for example).[3] Of particular interest is the possibility to do high-field DNP at low temperatures *in situ* to increase the sensitivity of magic-angle spinning (MAS) solid-state NMR spectroscopy.[4−6] While enhancements (ε) of 50 are today routinely obtained at 9.4 T and 100 K, allowing the investigation of an ever broader range of molecular systems including biomolecules and entire cells,[7−11] materials,[12−22] or bulk microcrystals,[23] the signal enhancement factors are still far from the predicted maximum values, and low sensitivity still prevents many potential applications.

Several factors affect enhancements since the trajectory of polarization from the unpaired electrons to the nuclei is complex, and the mechanism depends on parameters, such as the main magnetic field, the temperature of the sample, the nature of the propagating medium, or the concentration and structure of the species bearing the unpaired electrons (mostly organic free radical).[24,25] Here we focus on the initial transfer of polarization from electrons to nuclei. For this transfer at high-magnetic fields, the cross effect (CE) and thermal mixing (TM) are the most efficient mechanisms.[3,24] They are active when broadening of the EPR line width exceeds the nuclear Larmor frequency, and they involve a three-spin process including two dipolar coupled electron spins whose Larmor frequencies are separated by the nuclear Larmor frequency (the so-called matching condition).[3,26] To make this process as efficient as possible, over the last 10 years much effort has been devoted to the development of increasingly efficient exogenous polarizing agents. A major step was achieved by Griffin and co-workers who demonstrated in 2004 that biradicals with constrained $e-e$ distances, and thus increased $e-e$ dipolar couplings, yield more efficient CE DNP.[27] This has led to the introduction of stable nitroxide-based biradicals including TOTAPOL,[28] which is today the most commonly used polarization source for DNP solid-state NMR spectroscopy in aqueous media.

For nitroxide biradicals the matching condition is obtained for a given orientation through the **g** tensor anisotropy and can be fulfilled for the largest number of orientations when the two **g** tensors are nearly orthogonal. In 2009, Tordo, Griffin, and co-workers introduced the bTbK biradical[29] (Figure 1, **1**) for
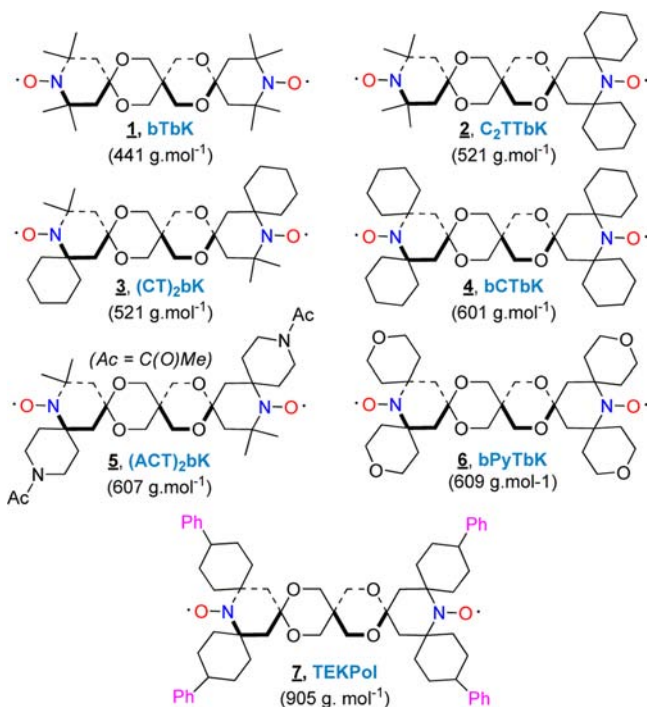

Figure 1. Structure, name, and molecular weight of the radicals investigated in this study.

which the orientation of the two **g** tensors is fixed by a rigid skeleton, leading to improved DNP efficiency when compared to more flexible radicals. This radical is soluble in a wide range of organic solvents compatible with DNP[30] and as such is well suited for applications to materials that are not compatible with water. Water-soluble rigid biradicals have been recently introduced, yielding enhancement factors higher than TOTA-POL in aqueous media.[31,32]

Beyond the geometry, the electronic relaxation properties of radical species are another key factor affecting the DNP process. Initial polarization transfer depends on saturation of an EPR transition, which is facilitated by longer electron spin relaxation times (T_{1e}, T_{2e}). For instance, it was shown in 2011 by Casabianca et al. that the efficiency of paramagnetic defects to polarize the bulk in nanoparticulate diamonds increased with increasing T_{1e}.[33] In 2012, our group introduced **2**, a bulky 2,6-spirocyclohexyl derivative of bTbK, dubbed bCTbK,[34] which has a long electron spin−lattice relaxation time and maintains optimal conformation for DNP. We showed that at 100 K this biradical has a T_{1e} twice as long as that of bTbK at 94 GHz and that this resulted in DNP enhancement factors up to 4 times larger. More recently it has been demonstrated that a mixture of narrow line radicals having differential electron spin−lattice relaxation times provides an effective alternative to biradicals for CE DNP to polarize carbon-13 directly.[35]

In this Article, we present a series of bTbK derivatives suitable for high-field DNP-enhanced solid-state NMR spectroscopy. We establish a clear relationship between the DNP efficiency of these new biradicals and their electronic relaxation

properties. In particular, a new dinitroxide radical **7**, TEKPol, is introduced that yields an unprecedented proton enhancement (ε_H) of over 200 at 9.4 T and 100 K in bulk solution as well as in mesoporous materials. The temperature and magic angle spinning (MAS) frequency behavior of the DNP enhancement factors is also discussed for this new family of polarizing agents.

■ EXPERIMENTAL SECTION

NMR Spectroscopy. DNP experiments were conducted on a commercial Bruker Avance III 400 MHz NMR spectrometer equipped with a 263 GHz gyrotron microwave source,[36] using a 3.2 mm triple resonance MAS probe at sample temperatures around 100 K (unless noted otherwise). The microwave power was set to maximize the DNP enhancement (∼4 W power at the sample). The magnet sweep coil was used to set the magnetic field to coincide with the maximum enhancement for TEKPol (which was found to be the same as for TOTAPOL, see Figure S1). Proton DNP enhancements were measured on spectra acquired after a short (1 rotor cycle) spin echo to remove probe background, and the enhancements of heteronuclei were measured after cross-polarization (CP) from protons. More details on the NMR parameters can be found in SI.

NMR Sample Preparation. The samples were either bulk solutions or mesoporous silica materials impregnated with biradical solution (prepared as previously described).[12,37] Samples were topped with a Teflon insert to minimize solvent leakage from the sapphire rotors. A spatula tip of KBr was added at the bottom of the rotor to enable measurement of ^{79}Br chemical shifts for temperature calibration.[38]

EPR Spectroscopy. Experiments were conducted at W Band (94 GHz) on a Bruker Elexsys E680 EPR spectrometer at a temperature of 100 K in tetrachloroethane (TCE), unless noted otherwise. The inversion recovery times (T_{ir}) were measured using an inversion−recovery sequence, and the data were fitted using a stretched exponential function. The phase memory times (T_m) were measured using a variable-delay Hahn echo pulse sequence and were fitted using a monoexponential function. Further details are given in SI.

To match the DNP conditions, samples were recorded at a high radical concentration (16 mM). For comparison, bTbK, bCTbK, and TEKPol were measured at low concentration (0.2, 0.1, and 0.1 mM, respectively). The results are discussed below.

Glass Formation. Experimentally, we observed variations (up to 80%) of the DNP enhancement in TCE solutions for some radicals upon freezing of the sample in the magnet. Several freezing and thawing cycles were performed by inserting and ejecting the sample from the probe. We report here the highest ε. Freezing the rotor in liquid nitrogen did not yield consistently better ε. The quality of the glass formed by freezing the sample is well-known to be an important factor for both DNP and EPR. Poor glasses or crystalline domains formed in the sample will lead to shortening of the relaxation times by creating zones of high local radical concentration, therefore attenuating the DNP process. This is why cryoprotectants, such as glycerol, are used in DNP experiments in water,[39] which crystallizes when frozen, or why alternative sample preparation schemes are being developed.[12,40] For samples yielding poor DNP enhancements, the ^{13}C NMR spectra display two shoulders due to residual coupling to chlorine. They might indicate formation of crystalline domains in the sample (see SI). In contrast reproducible enhancements were obtained when impregnating mesoporous materials.

EPR samples in small (0.5 mm) capillaries were frozen in liquid nitrogen prior measurement. Results were reproducible, and the samples were visually transparent and homogeneous, indicating glass formation.

Synthesis of the Materials. The mesoporous material used as a model here to evaluate surface NMR enhancements, Mat-Azide, was prepared as previously described.[34]

Synthesis of the Radicals. The general synthetic route to prepare compounds **1**−**7** involves three main steps which are illustrated in Figure 2 for TEKPol. Experimental details for reaction procedures and

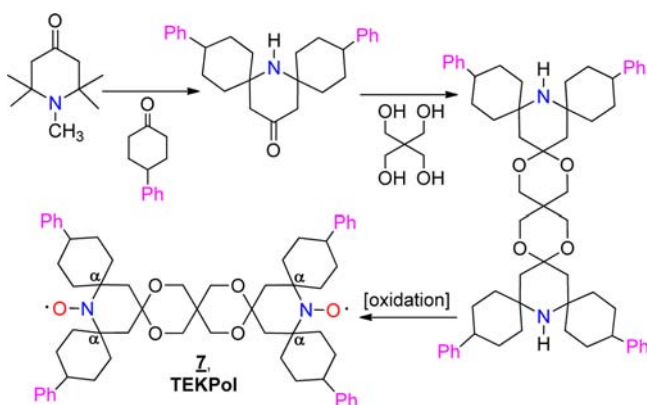characterization of all the new intermediates and biradicals are given in SI.

Figure 2. General synthetic route, illustrated for TEKPol, to synthesize compounds **1**−**7**.

RESULTS AND DISCUSSION

Longer Electronic Relaxation Times Are Expected to Yield More Efficient DNP at 9.4 T and 100 K. Efficiency of

the DNP process depends, as stated previously, on several parameters. The CE is a three spin (two electrons one nucleus) process that requires the saturation of one of the electron resonances to create a nonequilibrium state that then transfers polarization through a two-spin flip-flop of the other electron spin and the nuclear spin. The efficiency of the continuous-wave (CW) saturation of the electron spins depends on the saturation factor s ($s = T_{1e} \times T_{2e}$). The higher s, the more efficient the saturation will be.[41] We expect therefore that, if all the other parameters (**g** and **A** tensors, structure of the radicals, $e-e$ dipolar couplings) are almost constant, then the DNP efficiency of the radicals will increase with their saturation factors. In the following we develop radicals with improved saturation factors and thereby improved DNP performance. Figure 1 shows the chemical structure of the biradicals developed in this study, designed to provide longer electron relaxation times. The aim of this series is to access a range of radicals with the same EPR tensor parameters and relative orientations, the same electron−electron interactions, but with different electron spin relaxation properties. A synthetically feasible way to obtain such radicals is to modify the derivatives at α position (C_α) to the nitroxyl groups (N−O$^\bullet$) while maintaining the rest of the skeleton. The synthesis of such radicals is not always straightforward, and the spirocyclohexyl-
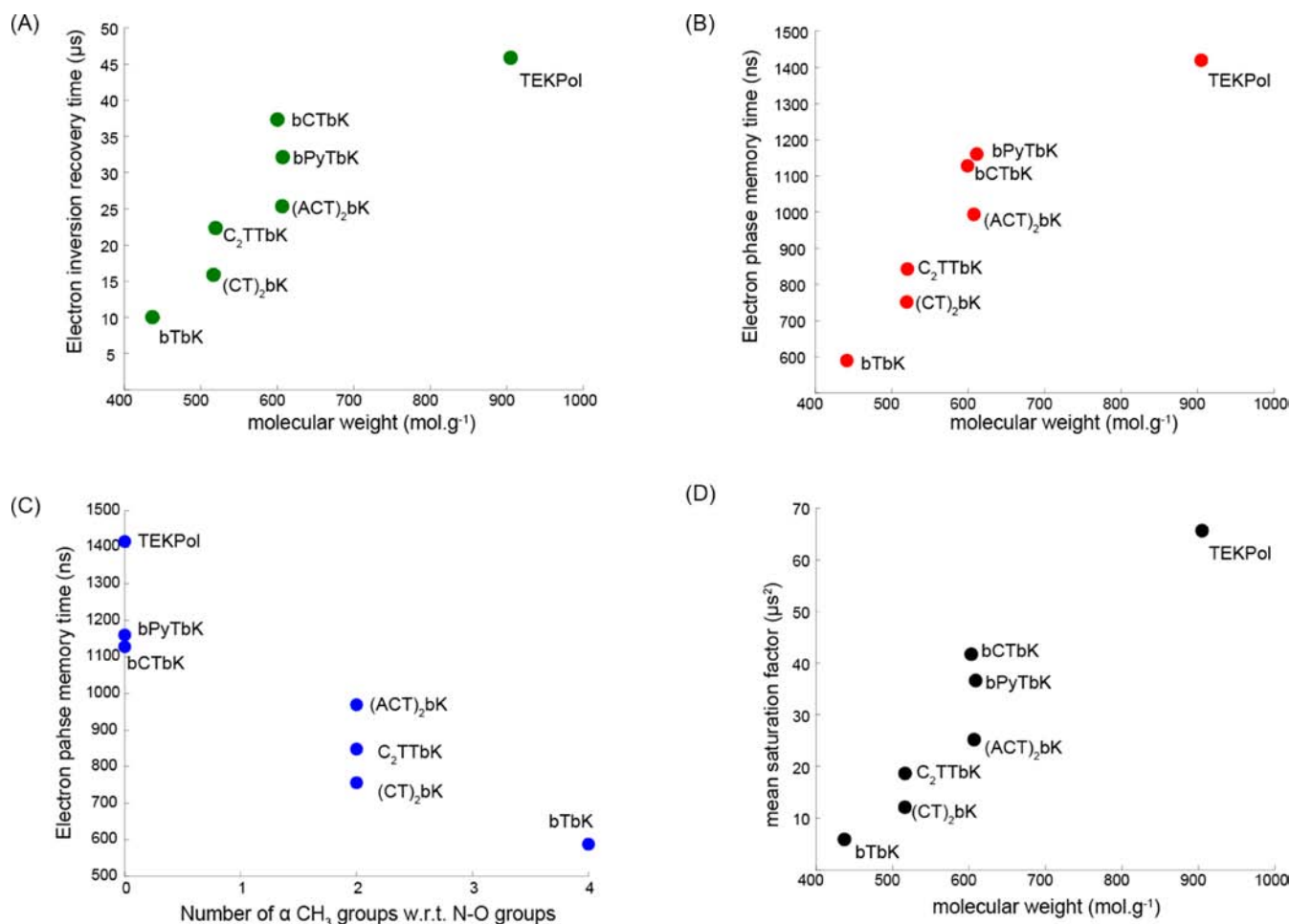

Figure 3. (A) Electron inversion recovery times (T_{ir}), (B) electron phase memory time (T_m) as a function of molecular weight for the different radicals, and (C) electron phase memory time (T_m) as a function of the number of methyl groups groups at the C_α carbons. (D) Saturation factor s as a function of molecular weight for the different radicals. (All measurements were done with 16 mM solutions in 1,1,2,2-TCE at 100 K. The EPR experiments are done at W band (94 GHz).

based functional groups used here were chosen due to reasonable yields. All the radicals of Figure 1 were prepared with the goal to cover a range of molecular weights.

Molecular Geometry and EPR Characterization of Biradicals 1–7. All these radicals have the same rigid trispiro backbone as bTbK and differ only in the substitution at the carbons in the α position (C_α) to the nitroxyl groups ($N-O^\bullet$) (Figure 2). Comparison of single crystal XRD (where available) or DFT calculations for **1**, **4**, **6**, and **7**, (Table S1), shows that as expected, the average distance between the two unpaired electrons (and thus the $e-e$ dipolar coupling) as well as the orientation of the two $C_\alpha N(O_\lambda)C_\alpha$ average planes are very similar throughout the series. In addition EPR spectra recorded at low temperature indicate that their **g** tensors are almost identical (see Figure S6).

Figure 3A,B shows the inversion recovery (T_{ir}) and phase memory (T_m) times measured for the radicals as a function of molecular weight. The experiment was performed near the ^{14}N $m_I = -1$ hyperfine component along $\mathbf{g}_{zz}$ of the EPR spectrum, corresponding to the optimum DNP irradiation frequency (as the relaxation times vary along the EPR powder pattern)[42] (see Figure S3). The biradical concentration in the solution for EPR was determined by CW EPR spin counting experiments and was found to vary between 11.0 and 14.7 mM. At these high concentrations, the measured inversion recovery and phase memory times do not correspond to the electron longitudinal and transverse relaxation times as intermolecular relaxation, such as spin exchange or dipolar coupling plays a role in the process.[43] We note however that these data are recorded under experimental conditions that are close to those used during the DNP experiments, and are thus the most relevant to our results. The most significant difference in conditions is the EPR frequency, which here is 94 GHz. However, the electron relaxation times of nitroxides in glassy organic solvents around 100 K are not expected to vary significantly between 94 and 263 GHz.[44] Thus the values reported here will not be exactly the same as those at the DNP frequencies (spectral diffusion will increase at higher fields), but they are expected to follow the same trends.[44] The inversion recovery curves were fitted using a stretched exponential function to take into account a distribution of inversion recovery time constants. T_m was fitted using a monoexponential function.

For radicals in glassy organic solvents around 100 K, the Raman process is expected to be the dominant mechanism of longitudinal relaxation for dilute samples. It has been shown that the efficiency of this two phonon process depends on the molecular weight of the radicals; the heavier the radical, the slower the relaxation. As spin diffusion leading to the spectral diffusion is driven by longitudinal relaxation, one still expects positive correlation between molecular weight and inversion recovery times at high concentrations.[42,44] The electron inversion recovery times (Figure 3A) measured for biradicals **1–7** show a roughly linear dependence on the molecular weight of the biradicals, as discussed in detail below.

At these temperatures, and in glassy solvents, T_m relaxation is governed by molecular motion and libration. Rotation of methyl groups, for instance, can induce effective transverse relaxation.[42] Replacing the methyl groups at C_α carbons by increasingly bulky and rigid functional groups is therefore expected to lengthen T_m.[45] Figure 3B,C shows, respectively, the impact of the molecular weight and of the number of methyl groups at C_α carbons on T_m. As expected, heavier radicals or radicals without methyl groups exhibit longer T_m.

Since molecular weight is not the only factor in determining relaxation times, some differences are observed in relaxation rates for radicals with similar molecular weight in Figure 3, as is demonstrated by **4** bCTbK, **5** (ACT)$_2$bK, and **6** bPyTbK. Sato et al. described electron spin relaxation for nitroxide radicals in glassy solvents at temperatures between 100 and 300 K using models that involved the corrected temperature $T' = TV^{-\gamma}$, where T is the temperature, V the molecular volume of the radical, and γ a parameter that characterizes the medium and is dependent on local molecular motion.[42] Their model predicts that bulkier radicals lead to slower relaxation and also that local motion affects relaxation. Furthermore for a biradical with interspin distance about 9 Å these authors showed[39] that nitroxide−nitroxide interaction has little impact on electron spin relaxation. Biradicals **4–6** have roughly the same molecular mass, but **5** has four methyl groups at the C_α carbons and two additional N-acetyl methyl groups. This is in line with the observation in Figure 3 that **4** has a shorter relaxation time than **6** which is in turn shorter than that for bCTbK. Measurements of T_{1e} and T_{2e} at low radical concentration were also carried out for bTbK, bCTbK, and TEKPol. The relaxation times at low concentration are found to be longer indicating that intermolecular dipolar relaxation occurs at 16 mM concentration, but as expected the trend remains the same, i.e. $T_{xe\ bTbK} < T_{xe\ bCTbK} < T_{xe\ bPhCTbK}$ (Figure S5).

As expected the mean saturation factor s ($s = T_{ir} * T_m$), which reflects the ability to saturate the EPR transitions, increases with molecular weight as shown in Figure 3D.

DNP Enhancements. Figure 4 shows the measured proton DNP enhancement of the solvent (measured on the carbon-13
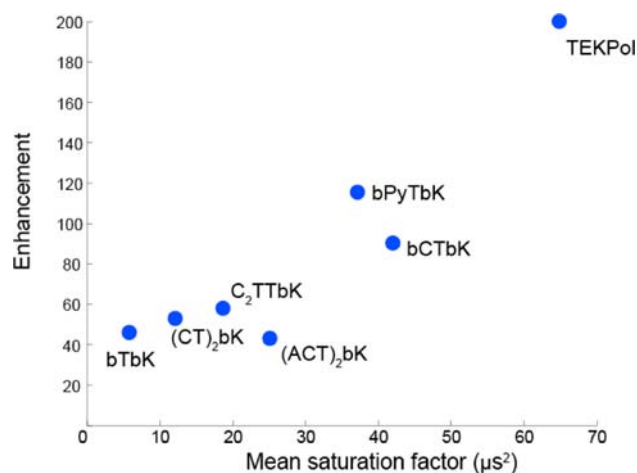

Figure 4. ^{13}C enhancement after CP from protons for 16 mM bulk solutions in TCE as a function of the mean saturation factor.

resonance of the solvent in a standard CPMAS experiment) obtained as a function of the mean saturation factor. As predicted, the DNP enhancement is seen to increase with the mean saturation factor and therefore with the molecular mass of the polarizing agent. In particular, TEKPol, with a molecular weight of 905 g·mol^{-1}, a 94 GHz mean saturation factor of 65.0 μs^2, and an enhancement of 200, far outperforms the other biradicals and notably the previous best bCTbK which gives an enhancement of 80. This is the highest enhancement presented for these conditions of temperature and field to date.

We note that it is expected that the DNP enhancement will go through a maximum at some point for higher saturation

factors. An optimum saturation factor is predicted since the degree of saturation of the EPR transition is improved at a given microwave power for larger saturation factors, whereas for repeated polarization transfer from the same electron spin to nuclei, the electron spin polarization must recover, so that shorter T_{ir} will increase turn over.[24] However, we only expect to see this effect for significantly longer electron relaxation times than studied here. For dinitroxides at the temperatures and fields used here we expect DNP enhancements to continue to increase with increasing saturation factors. Other types of radicals, such as mixed biradicals having radical moieties with one long T_{ir} and one short T_{ir} have been predicted to have high DNP enhancement.[24,35]

Temperature Dependence of DNP Enhancements. A key objective in the development of solid-state DNP experiments is to be able to use higher sample temperatures.[46] This is particularly relevant to proteins samples where resolution is often (but not always) degraded at temperatures below 200 K. ε is known to be strongly dependent on the temperature of the sample, with a steep decrease as temperature increases. Figure 5A shows the temperature dependence of ε for bTbK, bCTbK, and TEKPol. In these experiments, a spatula tip of crystalline KBr (which is insoluble in TCE) was added to the rotors, and the sample temperature was calibrated by using the ^{79}Br chemical shift as an internal standard.[38,47] As expected, ε decreases as the temperature increases for all three radicals. However, whereas bTbK exhibits the typical rapid decrease already observed for TOTAPOL in glycerol/water,[36] both bCTbK and TEKPol show a slower decrease with temperature over the range here. As a consequence, at around 140 K, ε is reduced by 60% from the value at 106 K for bTbK but only by 40% for both bCTbK and TEKPol. At around 176 K bTbK yields enhancements of only 4.5 ($\varepsilon/\varepsilon_{100K} = 0.16$), and bCTbK and TEKPol have ε of 24 ($\varepsilon/\varepsilon_{100K} = 0.25$) and 33 ($\varepsilon/\varepsilon_{100K} = 0.23$), respectively. Variation of the proton nuclear longitudinal relaxation time with temperature has been shown to affect the DNP enhancements.[36,39] However, for radical solutions in TCE, proton T_1 only varies slightly (from 2.0 to 2.6 s) in the range of temperature investigated (see SI). The temperature dependence of the enhancement can more credibly be linked to the temperature dependence of the electron relaxation times. As seen in Figure 4C, the saturation factors indeed decrease significantly with increasing temperature.

A key structural difference between bTbK and bCTbK or TEKPol is the presence of methyl groups at the C_α carbons of the former. Motion, and in particular the rotation of the methyl groups, is the dominant process for transverse relaxation, and the impact of temperature is therefore expected to be larger on T_m for bTbK than for the other radicals, which could explain the observed difference. Unfortunately, due to short T_m, measure of relaxation parameters could not be conducted at temperatures higher than 140 K for bTbK. This difference of behavior in T_m was previously observed for monoradicals with methyl groups at the C_α carbons vs radicals with cyclohexyls in the same position.[45,48] The individual temperature behavior of T_{ir} and T_m for the three radicals is given in Table S3. It is also interesting to note that the widely used radical TOTAPOL, which also has methyl groups at the C_α carbons has been reported to present a similar temperature dependence to that of bTbK.[36,49] Most interestingly, TEKPol maintains enhancements of 12 at 198 K.

MAS Frequency Dependence of ε. Another important parameter is the spinning frequency dependence of the
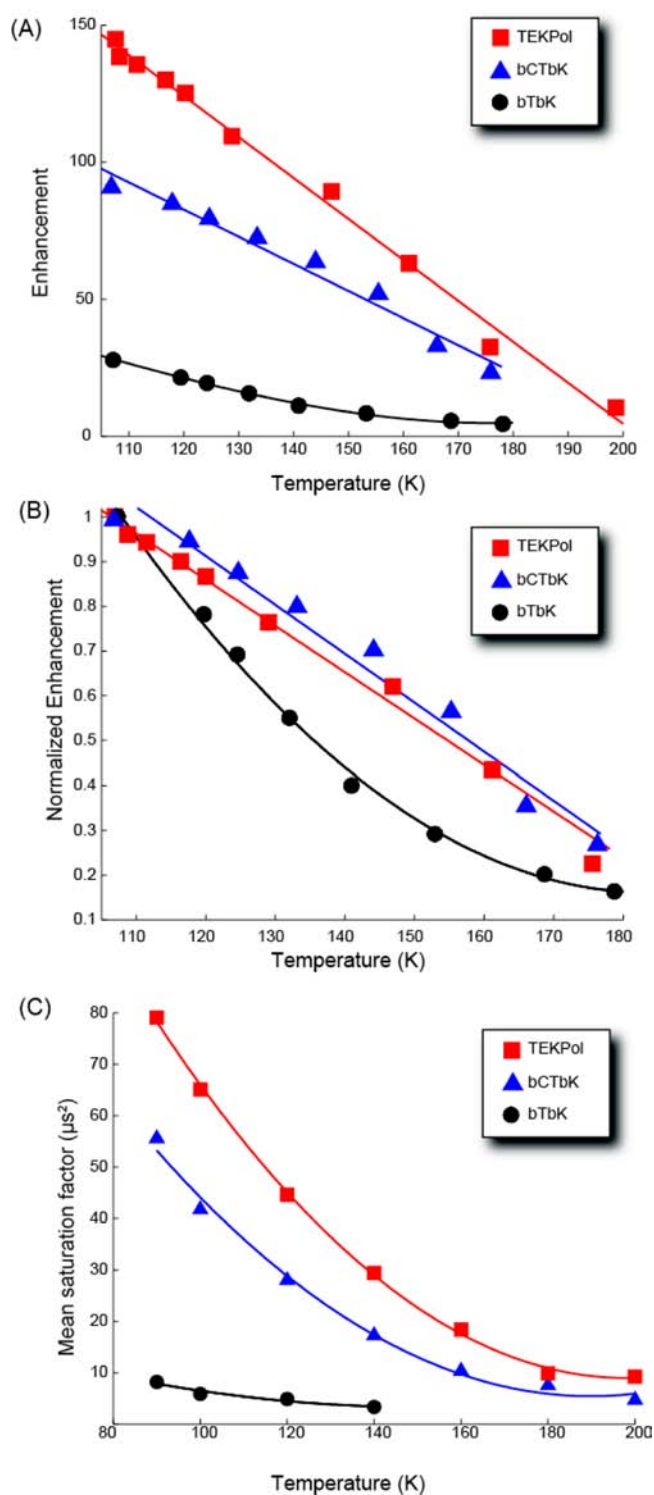

Figure 5. (A) Enhancement, (B) normalized enhancement, and (C) the mean saturation factor as a function of temperature for TEKPol (red squares), bCTbK (blue triangles), and bTbK (black circles). The lines are guides for the eye. Note that T_m becomes too short to detect an EPR echo at temperatures higher than 140 K.

enhancements. Fast spinning is essential for the study of many materials and biomolecules. The typical behavior for ε observed and reported with spinning frequency is first to increase and then go through a maximum (usually around 4 kHz spinning frequency) and then decrease as the spinning frequency increases to 12 kHz.[36] Rosay et al. attributed this

behavior primarily to an increase in sample temperature due to frictional heating with the spinning frequency.[36] More recently, Mentink-Vigier et al. and Thurber and Tycko developed a theoretical two-electron one-nucleus model for MAS CE DNP where the spinning frequency dependence is explained by energy level crossings and anticrossings.[50,51] We performed a temperature-controlled experiment for a 16 mM solution of TEKPol in TCE using the ^{79}Br chemical shift from KBr as an internal thermometer, as above. The ^{79}Br chemical shift was recorded at the highest spinning frequency (14 kHz), and for lower spinning frequencies the temperature control setting was increased so that the ^{79}Br chemical shift matches the one at 14 kHz. In this way, the experiments are carried out at the same temperature at all spinning frequencies. It turns out that the difference with respect to the spinning frequency dependence measured without correction for frictional heating is minor for the radical/solvent mixtures studied here. Figure 6 shows the spinning frequency dependence measured for the three radicals investigated.
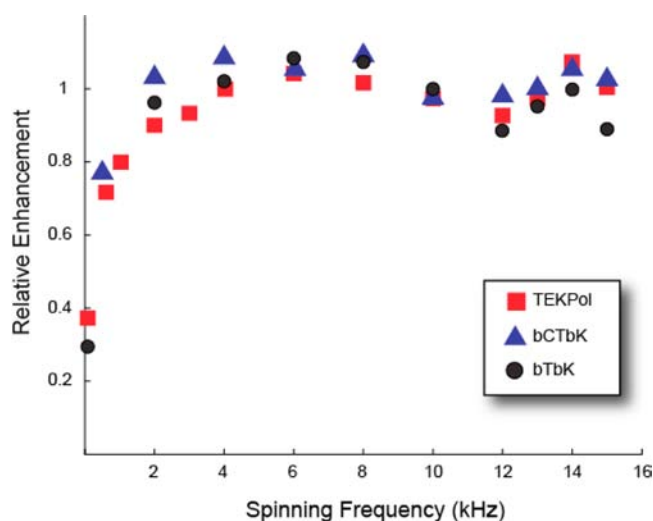

Figure 6. Relative enhancement dependence on the spinning frequency of the sample for TEKPol (red square), bCTbK (blue triangles), and bTbK (black circles).

For clarity, to compare the behavior, only the normalized enhancements are displayed. Interestingly, the curves show a decrease in efficiency from about 6 to 12 kHz, as expected, but they all then show an increase to a second maximum at around 14 kHz. We do not have an explanation for this interesting behavior. The three radicals show largely the same MAS dependence despite their different T_{1e}. The differences in T_{1e} may not be large enough to produce an observably different functional form.[50] Note that enhancements of over 160 are obtained at high spinning frequencies (15 kHz) for TEKPol.

Performance of the Radicals in Materials. One of the most recent applications of high-field DNP is the study of surfaces and materials.[12,13,15,17–22,34] In this approach, a material is impregnated with a minimal amount of the radical-containing solution. Interestingly, the material itself usually serves as a cryoprotectant and helps to form a good glass. DNP performance of the new radicals was investigated here for a mesoporous silica-containing propyl azide moieties bound to the silica surface via a C–Si linkage (**Mat-Azide**).[34] The results are summarized in Table 1. Along with ε, the quenching factor θ and the overall silicon enhancements $\sum$ are

Table 1. Bulk Solvent and Silicon Surface Enhancements, Quenching Factors, Overall Sensitivity Enhancements and Silicon Transverse Dephasing Times for 1 and 3−7

compound	$\varepsilon_{C\ CP}{}^{a}$ (bulk)	$\varepsilon_{Si\ CP}{}^{b}$ (mat)	$\theta_{Si}{}^{c}$	$\sum_{Si}{}^{d}$	$T_2'(^{29}Si)^{e}$ (ms)
bTbK, **1**	47	60	0.2	16	13
(CT)$_2$bK, **3**	53	80	0.2	25	5
bCTbK, **4**	80	103	0.2	35	14
(ACT)$_2$bK, **5**	42	32	0.6	13	29
bPyTbK, **6**	115	10	0.4	10	20
TEKPol, **7**	200	214	0.2	53	7

^{a}^{13}C enhancement measured on a bulk 16 mM TCE solution. ^{b}^{29}Si enhancement measured on **Mat-Azide** impregnated with a 16 mM TCE solution in. ^{c}^{29}Si quenching factor. ^{d}^{29}Si overall sensitivity enhancement. ^{e}^{29}Si transverse dephasing time.

reported.[37] θ is the fraction of nuclei that generate an observable signal at the surface of the mesoporous silica, and $\sum$ represents the overall gain in sensitivity, taking into account the quenching factor and modification in relaxation times between regular low temperature and DNP experiments.[37] For most of the radicals, ε increases in the materials as compared to the bulk solution, consistent with previous observations and with the cryoprotecting role of the material.[34] There are two notable exceptions: **5** and **6**, where ε drops from 42 to 32 and from 115 to 10, respectively. This can potentially be attributed to the differences in polarity among the radicals that causes them to interact differently with the surface. Differences in surface−radical interactions depending on the polarity of the surface were observed in a previous DNP study.[52] Wessig et al. showed by EPR that matching the polarity of the solvent and the surface minimizes radical−surface interactions.[53] This hypothesis is supported here by the measure of the ^{29}Si transverse dephasing time (T_2'), which is a good sensor of the proximity of the radicals to the surface silicon atoms. For the other radicals T_2' is shorter than 14 ms, but it increases to 20 ms for **6** and to 29 ms for **5**, indicating that in these cases the radical is further away from the surface, for example, through a partial exclusion from the pores thereby explaining the reduction in DNP efficiency.

■ CONCLUSION

The study of the effect of electron spin relaxation times on DNP enhancements for a series of bTbK analogs leads us to establish clear design principles for efficient dinitroxide biradicals. The structure and thus the **g** and **A** tensors as well as the $e−e$ dipole couplings of these derivatives are very similar, and therefore the main differences in observed DNP efficiency are attributed to electron relaxation properties of the radicals. The saturation factor of the electron spin transitions was found to be highly correlated with the DNP enhancements. Dinitroxide biradicals which have high molecular weights (large rigid volumes) and no methyl groups close to the nitroxyl groups (N−O$^{\bullet}$) are predicted to have high DNP efficiency.

A new heavy analog of bTbK, TEKPol is shown to yield proton polarization enhancements of over 200 at 9.4 T and 100 K, both for bulk and materials applications, and is the most efficient polarizing agent found so far for these conditions.

Furthermore, TEKPol retains high enhancements at higher temperatures, here providing $\sum$ = 33 at 180 K and 12 at 200 K. It also provides substantial enhancements at high MAS

12795

dx.doi.org/10.1021/ja405813t | *J. Am. Chem. Soc.* 2013, 135, 12790−12797

frequencies (over 150 at 15 kHz). We expect that water-soluble derivatives of this biradical, or more generally water-soluble dinitroxide biradicals with bulky substituents and no methyl groups at the C_α carbons, will retain high enhancements at high temperatures and high spinning frequencies, thus opening up the perspective of achieving higher resolution DNP spectroscopy in biosolids, currently one of the main drawbacks of CE DNP in biological applications.

■ ASSOCIATED CONTENT

ⓢ Supporting Information

Additional experimental details of preparation of materials and radicals, measurement of quenching and enhancement factors, impact of the number of methyl groups and of temperature on the relaxation times, comparison of relaxation times at high and low concentration, and detailed MAS curves are available. This material is available free of charge via the Internet at http://pubs.acs.org.

■ AUTHOR INFORMATION

Corresponding Author

paul.tordo@univ-amu.fr; lyndon.emsley@ens-lyon.fr

Notes

The authors declare no competing financial interest.

■ ACKNOWLEDGMENTS

■ REFERENCES

(1) Overhauser, A. *Phys. Rev.* **1953**, *92*, 411–415.
(2) Carver, T. *Phys. Rev.* **1956**, *102*, 975–981.
(3) Maly, T.; Debelouchina, G. T.; Bajaj, V. S.; Hu, K.-N.; Joo, C.-G.; Mak Jurkauskas, M. L.; Sirigiri, J. R.; van der Wel, P. C. A.; Herzfeld, J.; Temkin, R. J.; Griffin, R. G. *J. Chem. Phys.* **2008**, *128*, 052211.
(4) Becerra, L.; Gerfen, G.; Temkin, R.; Singel, D.; Griffin, R. *Phys. Rev. Lett.* **1993**, *71*, 3561–3564.
(5) Gerfen, G.; Becerra, L.; Hall, D.; Griffin, R. *J. Chem. Phys.* **1995**, *102*, 9494–9496.
(6) Rosay, M.; Lansing, J. C.; Haddad, K. C.; Bachovchin, W. W.; Herzfeld, J.; Temkin, R. J.; Griffin, R. G. *J. Am. Chem. Soc.* **2003**, *125*, 13626–13627.
(7) Andreas, L. B.; Barnes, A. B.; Corzilius, B.; Chou, J. J.; Miller, E. A.; Caporini, M.; Rosay, M.; Griffin, R. G. *Biochemistry* **2013**, *52*, 2774–2782.
(8) Sergeyev, I. V.; Day, L. A.; Goldbourt, A.; McDermott, A. E. *J. Am. Chem. Soc.* **2011**, *133*, 20208–20217.
(9) Renault, M.; Pawsey, S.; Bos, M. P.; Koers, E. J.; Nand, D.; Tommassen-van Boxtel, R.; Rosay, M.; Tommassen, J.; Maas, W. E.; Baldus, M. *Angew. Chem., Int. Ed.* **2012**, *51*, 2998–3001.
(10) Takahashi, H.; Ayala, I.; Bardet, M.; De Paëpe, G.; Simorre, J.-P.; Hediger, S. *J. Am. Chem. Soc.* **2013**, *135*, 5105–5110.
(11) Jacso, T.; Franks, W. T.; Rose, H.; Fink, U.; Broecker, J.; Keller, S.; Oschkinat, H.; Reif, B. *Angew. Chem., Int. Ed.* **2012**, *51*, 432–435.
(12) Lesage, A.; Lelli, M.; Gajan, D.; Caporini, M. A.; Vitzthum, V.; Miéville, P.; Alauzun, J.; Roussey, A.; Thieuleux, C.; Mehdi, A.; Bodenhausen, G.; Copéret, C.; Emsley, L. *J. Am. Chem. Soc.* **2010**, *132*, 15459–15461.

(13) Lelli, M.; Gajan, D.; Lesage, A.; Caporini, M. A.; Vitzthum, V.; Miéville, P.; Héroguel, F.; Rascón, F.; Roussey, A.; Thieuleux, C.; Boualleg, M.; Veyre, L.; Bodenhausen, G.; Copéret, C.; Emsley, L. *J. Am. Chem. Soc.* **2011**, *133*, 2104–2107.
(14) Lafon, O.; Rosay, M.; Aussenac, F.; Lu, X.; Trébosc, J.; Cristini, O.; Kinowski, C.; Touati, N.; Vezin, H.; Amoureux, J.-P. *Angew. Chem., Int. Ed.* **2011**, *50*, 8367–8370.
(15) Rossini, A. J.; Zagdoun, A.; Lelli, M.; Canivet, J.; Aguado, S.; Ouari, O.; Tordo, P.; Rosay, M.; Maas, W. E.; Copéret, C.; Farrusseng, D.; Emsley, L.; Lesage, A. *Angew. Chem., Int. Ed.* **2012**, *51*, 123–127.
(16) Vitzthum, V.; Miéville, P.; Carnevale, D.; Caporini, M. A.; Gajan, D.; Copéret, C.; Lelli, M.; Zagdoun, A.; Rossini, A. J.; Lesage, A.; Emsley, L.; Bodenhausen, G. *Chem. Commun.* **2012**, *48*, 1988–1990.
(17) Lafon, O.; Thankamony, A. S. L.; Kobayashi, T.; Carnevale, D.; Vitzthum, V.; Slowing, I. I.; Kandel, K.; Vezin, H.; Amoureux, J.-P.; Bodenhausen, G.; Pruski, M. *J. Phys. Chem. C* **2013**, *117*, 1375–1382.
(18) Lee, D.; Takahashi, H.; Thankamony, A. S. L.; Dacquin, J.-P.; Bardet, M.; Lafon, O.; Paëpe, G. D. *J. Am. Chem. Soc.* **2012**, *134*, 18491–18494.
(19) Blanc, F.; Sperrin, L.; Jefferson, D. A.; Pawsey, S.; Rosay, M.; Grey, C. P. *J. Am. Chem. Soc.* **2013**, *135*, 2975–2978.
(20) Samantaray, M. K.; Alauzun, J.; Gajan, D.; Kavitake, S.; Mehdi, A.; Veyre, L.; Lelli, M.; Lesage, A.; Emsley, L.; Copéret, C.; Thieuleux, C. *J. Am. Chem. Soc.* **2013**, *135*, 3193–3199.
(21) Grüning, W. R.; Rossini, A. J.; Zagdoun, A.; Gajan, D.; Lesage, A.; Emsley, L.; Copéret, C. *Phys. Chem. Chem. Phys.* **2013**, *15*, 13270–13274.
(22) Rossini, A. J.; Zagdoun, A.; Lelli, M.; Lesage, A.; Copéret, C.; Emsley, L. *Acc. Chem. Res.* **2013**, DOI: 10.1021/ar300322x.
(23) Rossini, A. J.; Zagdoun, A.; Hegner, F.; Schwarzwälder, M.; Gajan, D.; Copéret, C.; Lesage, A.; Emsley, L. *J. Am. Chem. Soc.* **2012**, *134*, 16899–16908.
(24) Hu, K.-N. *Solid State Nucl. Magn. Reson.* **2011**, *40*, 31–41.
(25) Ni, Q. Z.; Daviso, E.; Can, T. V.; Markhasin, E.; Jawla, S. K.; Swager, T. M.; Temkin, R. J.; Herzfeld, J.; Griffin, R. G. *Acc. Chem. Res.* **2013**, DOI: 10.1021/ar300348n.
(26) Hovav, Y.; Feintuch, A.; Vega, S. *J. Magn. Reson.* **2012**, *214*, 29–41.
(27) Hu, K.-N.; Yu, H.-H.; Swager, T. M.; Griffin, R. G. *J. Am. Chem. Soc.* **2004**, *126*, 10844–10845.
(28) Song, C.; Hu, K.-N.; Joo, C.-G.; Swager, T. M.; Griffin, R. G. *J. Am. Chem. Soc.* **2006**, *128*, 11385–11390.
(29) Matsuki, Y.; Maly, T.; Ouari, O.; Karoui, H.; Le Moigne, F.; Rizzato, E.; Lyubenova, S.; Herzfeld, J.; Prisner, T.; Tordo, P.; Griffin, R. G. *Angew. Chem., Int. Ed.* **2009**, *48*, 4996–5000.
(30) Zagdoun, A.; Rossini, A. J.; Gajan, D.; Bourdolle, A.; Ouari, O.; Rosay, M.; Maas, W. E.; Tordo, P.; Lelli, M.; Emsley, L.; Lesage, A.; Copéret, C. *Chem. Commun.* **2012**, *48*, 654–656.
(31) Dane, E. L.; Corzilius, B.; Rizzato, E.; Stocker, P.; Maly, T.; Smith, A. A.; Griffin, R. G.; Ouari, O.; Tordo, P.; Swager, T. M. *J. Org. Chem.* **2012**, *77*, 1789–1797.
(32) Kiesewetter, M. K.; Corzilius, B.; Smith, A. A.; Griffin, R. G.; Swager, T. M. *J. Am. Chem. Soc.* **2012**, *134*, 4537–4540.
(33) Casabianca, L. B.; Shames, A. I.; Panich, A. M.; Shenderova, O.; Frydman, L. *J. Phys. Chem. C* **2011**, *115*, 19041–19048.
(34) Zagdoun, A.; Casano, G.; Ouari, O.; Lapadula, G.; Rossini, A. J.; Lelli, M.; Baffert, M.; Gajan, D.; Veyre, L.; Maas, W. E.; Rosay, M.; Weber, R. T.; Thieuleux, C.; Copéret, C.; Lesage, A.; Tordo, P.; Emsley, L. *J. Am. Chem. Soc.* **2012**, *134*, 2284–2291.
(35) Michaelis, V. K.; Smith, A. A.; Corzilius, B.; Haze, O.; Swager, T. M.; Griffin, R. G. *J. Am. Chem. Soc.* **2013**, *135*, 2935–2938.
(36) Rosay, M.; Tometich, L.; Pawsey, S.; Bader, R.; Schauwecker, R.; Blank, M.; Borchard, P. M.; Cauffman, S. R.; Felch, K. L.; Weber, R. T.; Temkin, R. J.; Griffin, R. G.; Maas, W. E. *Phys. Chem. Chem. Phys.* **2010**, *12*, 5850.
(37) Rossini, A. J.; Zagdoun, A.; Lelli, M.; Gajan, D.; Rascón, F.; Rosay, M.; Maas, W. E.; Copéret, C.; Lesage, A.; Emsley, L. *Chem. Sci.* **2012**, *3*, 108–115.

(38) Thurber, K. R.; Tycko, R. *J. Magn. Reson.* **2009**, *196*, 84−87.

(39) Rosay, M. Ph.D. Thesis, *Massachuchetts Institute of Technology*, Cambridge, MA, 2001.

(40) Ravera, E.; Corzilius, B.; Michaelis, V. K.; Rosa, C.; Griffin, R. G.; Luchinat, C.; Bertini, I. *J. Am. Chem. Soc.* **2013**, *135*, 1641−1644.

(41) Weil, J. A.; Bolton, J. R. *Electron Paramagnetic Resonance*; Wiley-Interscience: Hoboken, NJ, 2007.

(42) Sato, H.; Kathirvelu, V.; Fielding, A.; Blinco, J. P.; Micallef, A. S.; Bottle, S. E.; Eaton, S. S.; Eaton, G. R. *Mol. Phys.* **2007**, *105*, 2137−2151.

(43) Sato, H.; Kathirvelu, V.; Spagnol, G.; Rajca, S.; Rajca, A.; Eaton, S. S.; Eaton, G. R. *J. Phys. Chem. B* **2008**, *112*, 2818−2828.

(44) Eaton, S.; Harbridge, J.; Rinard, G.; Eaton, G.; Weber, R. *Appl. Magn. Reson.* **2001**, *20*, 151−157.

(45) Kathirvelu, V.; Smith, C.; Parks, C.; Mannan, M. A.; Miura, Y.; Takeshita, K.; Eaton, S. S.; Eaton, G. R. *Chem. Commun. (Camb.)* **2009**, 454−456.

(46) Akbey, Ü.; Linden, A. H.; Oschkinat, H. *Appl. Magn. Reson.* **2012**, *43*, 81−90.

(47) Miéville, P.; Vitzthum, V.; Caporini, M. A.; Jannin, S.; Gerber-Lemaire, S.; Bodenhausen, G. *Magn. Reson. Chem.* **2011**, *49*, 689−692.

(48) Rajca, A.; Kathirvelu, V.; Roy, S. K.; Pink, M.; Rajca, S.; Sarkar, S.; Eaton, S. S.; Eaton, G. R. *Chemistry* **2010**, *16*, 5778−5782.

(49) Akbey, Ü.; Franks, W. T.; Linden, A.; Lange, S.; Griffin, R. G.; van Rossum, B.-J.; Oschkinat, H. *Angew. Chem., Int. Ed.* **2010**, *49*, 7803−7806.

(50) Mentink-Vigier, F.; Akbey, Ü.; Hovav, Y.; Vega, S.; Oschkinat, H.; Feintuch, A. *J. Magn. Reson.* **2012**, *224*, 13−21.

(51) Thurber, K. R.; Tycko, R. *J. Chem. Phys.* **2012**, *137*, 084508.

(52) Zagdoun, A.; Rossini, A. J.; Conley, M. P.; Grüning, W. R.; Schwarzwälder, M.; Lelli, M.; Franks, W. T.; Oschkinat, H.; Copéret, C.; Emsley, L.; Lesage, A. *Angew. Chem., Int. Ed.* **2013**, *52*, 1222−1225.

(53) Wessig, M.; Drescher, M.; Polarz, S. *J. Phys. Chem. C* **2013**, *117*, 2805−2816.